4-O-Substituted Glucuronic Cyclophellitols are Selective Mechanism-Based Heparanase Inhibitors

Valentina Borlandelli,[a] Zachary Armstrong,[a, b] Alba Nin-Hill,[c] Jeroen D. C. Codée,[a] Lluís Raich,[c, d] Marta Artola,[a] Carme Rovira,[c] Gideon J. Davies,*[b] and Herman S. Overkleeft*[a]

Degradation of the extracellular matrix (ECM) supports tissue integrity and homeostasis, but is also a key factor in cancer metastasis. Heparanase (HPSE) is a mammalian ECM-remodeling enzyme with β-D-endo-glucuronidase activity overexpressed in several malignancies, and is thought to facilitate tumor growth and metastasis. By this virtue, HPSE is considered an attractive target for the development of cancer therapies, yet to date no HPSE inhibitors have progressed to the clinic. Here we report on the discovery of glucurono-configured cyclitol derivatives featuring simple substituents at the 4-O-position as irreversible HPSE inhibitors. We show that these compounds, unlike glucurono-cyclophellitol, are selective for HPSE over β-D-exo-glucuronidase (GUSB), also in platelet lysate. The observed selectivity is induced by steric and electrostatic interactions of the substituents at the 4-O-position. Crystallographic analysis supports this rationale for HPSE selectivity, and computer simulations provide insights in the conformational preferences and binding poses of the inhibitors, which we believe are good starting points for the future development of HPSE-targeting antimetastatic cancer drugs.

Introduction

Heparan sulfate (HS) is a polyanionic glycosaminoglycan (GAG) present in the extracellular matrix (ECM) and in the basal membrane of mammalian cells. Covalently linked to cell-surface and extracellular matrix proteins, HS is an integral part of heparan sulfate proteoglycans (HSPGs),[1] fundamental glycoproteins in maintaining tissue integrity and transduction of cell signaling.[2] HS (Figure 1A) features a heterogeneous sulfation pattern, which provides binding sites for various ligands, such as growth factors, cytokines and amyloid β (Aβ) peptides. This interaction with its binding partners is thought to account for
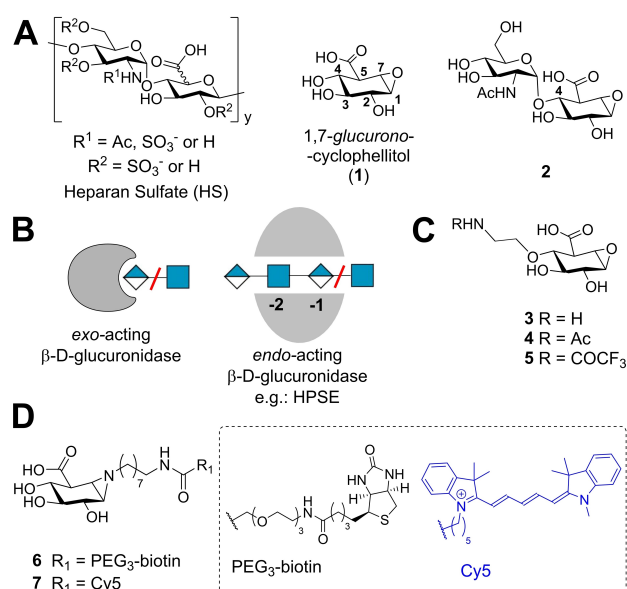
Figure 1. (A) Chemical structures of heparan sulfate, 1,7-glucurono-cyclophellitol **1** and disaccharidic 1,67-glucurono-cyclophellitol **2**. (B) Schematic difference between exo- and endo-acting retaining β-D-glucuronidases. Design of mechanism-based heparanase inhibitors **3–5** (C) and of ABPs **6–7** (D) acting on both exo and endo retaining β-D-glucuronidases.

[a] V. Borlandelli, Dr. Z. Armstrong, Dr. J. D. C. Codée, Dr. M. Artola, Prof. H. S. Overkleeft
Bio-organic Synthesis, Leiden Institute of Chemistry (LIC)
Leiden University, Gorlaeus Laboratories
Einsteinweg 55, 2333 CC Leiden (The Netherlands)
E-mail: h.s.overkleeft@lic.leidenuniv.nl

[b] Dr. Z. Armstrong, Prof. G. J. Davies
Department of Chemistry, York Structural Biology Laboratory
University of York, Heslington, YO10 5DD York (UK)
E-mail: gideon.davies@york.ac.uk

[c] Dr. A. Nin-Hill, Dr. L. Raich, Prof. C. Rovira
Departament de Química Inorgànica i Orgànica (Secció de Química Orgànica) and Institut de Química Teòrica i Computacional (IQTCUB)
Universitat de Barcelona
Martí i Franquès 1, 08028 Barcelona (Spain)

[d] Dr. L. Raich
Current address:
Department of Mathematics and Computer Science
Freie Universität Berlin, 14195 Berlin (Germany)

Supporting information for this article is available on the WWW under https://doi.org/10.1002/cmdc.202200580

the roles of HSPGs in (patho)physiological processes, and that include cell signaling, endocytosis and cell adhesion.

In mammals, HSPGs are a major constituent of the extracellular matrix (ECM), which undergoes substantial compositional and structural changes during cancer growth and metastasis[3] as a result of the activity of several enzymes. Among the ECM-remodeling enzymes, heparanase (HPSE) is the mammalian endo-acting β-D-glucuronidase (Figure 1B) respon-

ChemMedChem

Research Article
doi.org/10.1002/cmdc.202200580

Chemistry Europe
European Chemical
Societies Publishing

sible for cleaving HS chains from HSPGs (Figure 2A). The enzyme is expressed as an inactive pro-enzyme (proHPSE), and matures into the active form by proteolytic cleavage of an 8 kDa linker peptide.[4] In primary metastatic cancers, HPSE overexpression[5] drives dysregulated degradation of the ECM, which in turn facilitates cancer cell proliferation, oncogenic signaling[6,7] and angiogenesis.[8,9] In this way, HPSE contributes to tumor growth and metastasis and consequently, HPSE has emerged as a potential therapeutic target. One approach to modulate HPSE activity is by inhibition of its enzymatic activity. In this respect, four competitive HPSE inhibitors have been subjected to clinical studies.[10–13] None have made it to the clinic yet which may be due to their non-drug-like properties: all these inhibitors are large, heterogeneous and charged HS-mimicking oligosaccharides.[14] Other HPSE inhibitor designs include azasugars,[15–17] nucleic acid derivatives,[18] and non-sugar small-molecule compounds,[19,20] all designed as competitive inhibitors. Because the HPSE binding site accommodates extensive interactions with large HS oligosaccharide substrates, small-molecule competitive inhibitors with high affinity are difficult to access. This does not necessarily hold true for mechanism-based, covalent and irreversible inhibitors: even if initial binding affinity is modest, efficient reaction with an enzyme active site residue to form a covalent and irreversible bond will lead to efficient overall enzyme inactivation (Figure 2B). We have shown this to be true in our previous report on *glucurono*-configured cyclophellitol (**1**, Figure 1A), a potent

inhibitor of retaining *exo*-acting β-D-glucuronidases.[21] Surprisingly and although less potent, compound **1** proved also able to inactivate human HPSE. Capitalizing on this result and with the potential use of HPSE inhibitors as antitumor agents in mind, we then evaluated the potency and selectivity of 4-*O*-GlcNAc-*glucurono*-cyclophellitol **2** (Figure 1A),[22] which proved to be both a more potent and a much more selective HPSE inhibitor compared to *exo*-acting β-D-glucuronidases. In this work we further explore the viability of substituted glucuronic cyclophellitols as selective HPSE inhibitors. Specifically, our aim was to establish whether substituting the GlcNAc moiety in **2** for structurally smaller functionalities would yield compounds retaining the activity and selectivity profile of **2**, and possibly yet more drug-like molecules, as in compounds **3**–**5** (Figure 1C). We here show that compounds **4** and **5** (but not amine derivative **3**) are indeed micromolar inactivators of HPSE with superior HPSE selectivity compared to unsubstituted *glucurono*-configured cyclophellitol (**1**).

To assist in the analysis of (substituted) glucuronic cyclophellitols on their potency and selectivity as inhibitors of *endo*- and *exo*-acting β-D-glucuronidases we also developed activity-based probes (ABPs) **6** and **7** (Figure 1D), which are more chemically accessible than the ones we published previously.[15] Altogether, with compounds **4** and **5** as attractive starting points for further exploring the chemical space around the glucuronic cyclophellitol core, and with the accompanying activity-based protein profiling (ABPP) assays based on ABPs **6**
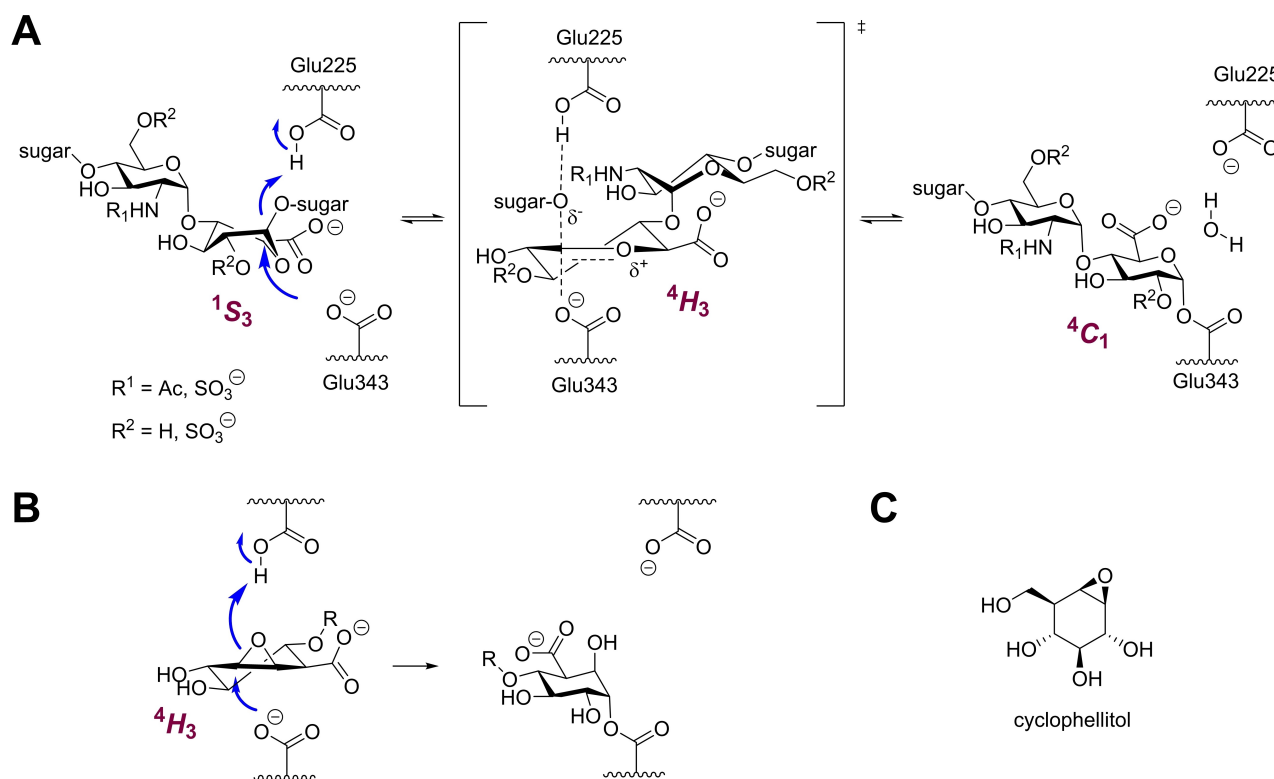
Figure 2. (**A**) HS processing by HPSE proceeds through the formation of a transient covalent enzyme-substrate acylal adduct employing a $^1S_3$–$^4H_3$–$^4C_1$ conformational itinerary. (**B**) Schematic representation of the inactivation mechanism for HPSE by substituted glucuronic cyclophellitols. Upon nucleophilic attack, a stable enzyme-inhibitor ester adduct is formed. (**C**) Chemical structure of cyclophellitol.

ChemMedChem

Research Article
doi.org/10.1002/cmdc.202200580

**Chemistry Europe**
European Chemical
Societies Publishing

and **7** in place, our work as presented here may assist in finding much sought-after commodities in anticancer drug discovery: small molecule, potent and selective HPSE inhibitors.

Results and Discussion

Design and synthesis

To define the likely conformation of inhibitors **3–5** when entering the enzyme active sites, we calculated the relative energy for all ring conformations of unsubstituted *glucurono*-cyclophellitol *in vacuo* (Figure 3). HPSE, like GS1 retaining β-glucosidases, process their substrate through a $^{1}S_{3}$–$^{4}H_{3}$–$^{4}C_{1}$ reaction itinerary (Figure 2A).[23] The prototype mechanism-based retaining glycosidase inhibitor, cyclophellitol, potently and irreversibly inhibits retaining β-glucosidases[24] by mimicking the $^{4}H_{3}$ transition state (TS) conformation when bound in the active site,[25] after which nucleophilic opening of the epoxide occurs. This TS conformation is indeed the preferred conformation of free cyclophellitol as revealed by the calculated free energy landscape (FEL) (Figure S1). The FEL calculations were performed using *ab initio* metadynamics[26] with the Cremer-Pople puckering coordinates for monocyclic rings as collective variables.[27] Similar to cyclophellitol, *glucurono*-cyclophellitol also adopts this preferred $^{4}H_{3}$ TS conformation in FEL calculations (Figure 3A), which is consistent with its efficient binding to the HPSE active site, and also that of retaining β-exoglucosidases.

The design of **3–5** was done as follows. We reasoned that modification at *O*-4 would not significantly influence the conformation of the glucuronic cyclophellitol ring. The corresponding FEL calculation of unsubstituted glucuronic cyclophellitol shows that all thermally accessible ring conformations are in an energy window of approximately 7 kcal/mol, in line
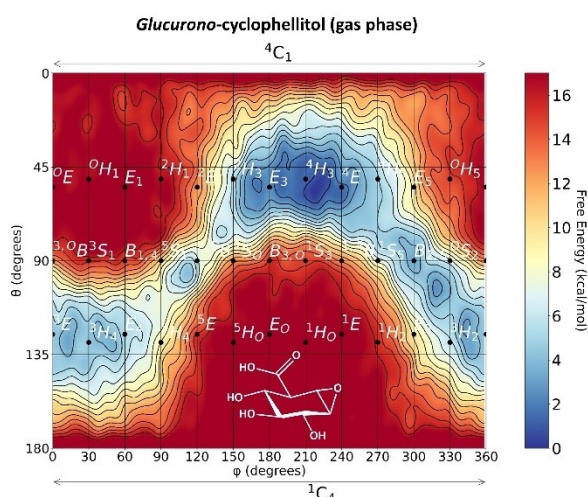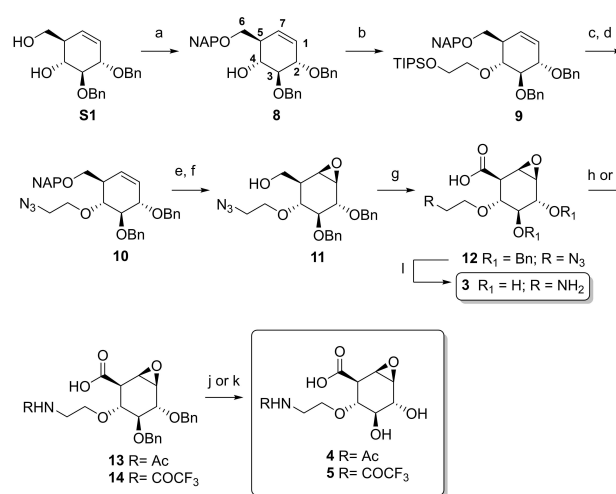
with findings on pyranose-based compounds.[28] Small differences are observed between the two computed FELs in terms of their local energy minima.

With respect to the selected *O*-4-substituents, we reasoned that substitution of the GlcNAc moiety in **2** with an *N*-acetyl-aminoethyl moiety would yield a compound (**3**, Figure 1C) that should still bind to HPSE (the acetylaminoethyl ether can be viewed as a minimal GlcNAc residue still featuring the acetamide) but that, due to the *O*-4-substituent, is not able to access the active site of *exo*-acting β-D-glucuronidases.
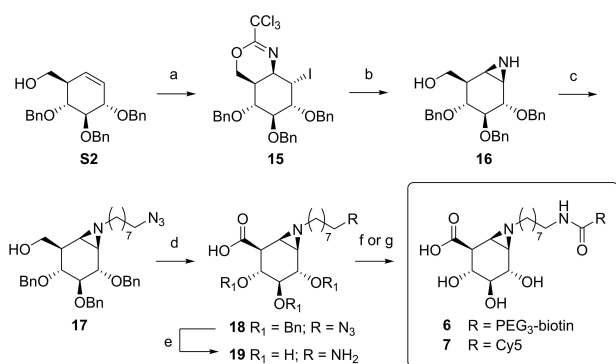
Compound **4**, the corresponding trifluoroacetamide **5** and free amine **3** (the latter two selected to probe the contribution of the acetamide to HPSE inhibition) were prepared from *gluco*-configured cyclohexene **S1**[29] as depicted in Scheme 1. The primary alcohol in **S1** was selectively naphthylated, yielding compound **8** with 4-OH available for functionalization. 4-*O*-alkylation of **8** allowed to install an *O*-silyl-protected ethylene fragment for further derivatization. Desilylation of intermediate **9** gave the corresponding primary alcohol, which was then tosylated and subsequently treated with sodium azide to give common intermediate **10**. Removal of the naphthyl protecting group in **10** and subsequent stereoselective epoxidation with *m*-CPBA generated epoxide **11** with the desired stereochemistry by participation of the primary alcohol. Oxidation of the primary alcohol in **11** into the carboxylate with 2,2,6,6-tetramethylpiperidine-1-oxyl radical (TEMPO)/bis-acetoxyiodobenzene (BAIB) according to the protocol of Epp and Widlansky[30] at 0 °C resulted in common intermediate **12**, from which the three target inhibitors derived. Zinc-mediated azide reduction followed by *N*-acetylation or *N*-trifluoroacetylation yielded **13** and **14**, respectively. Hydrogenolytic debenzylation of these with

Figure 3. Gas-phase free-energy landscapes of *glucurono*-cyclophellitol. The *glucurono*-cyclitol adopts a $^{4}H_{3}$ ground-state conformation. The *x* and *y* axes correspond to the φ and ϑ Cremer-Pople puckering coordinates, respectively. Isolines are 1 kcal/mol.

Scheme 1. Reagents and conditions: (a) i. NapBr, KI, K$_2$CO$_3$, 2-aminoethyl-diphenylborrate, CH$_3$CN, 88%. (b) TIPSO(CH$_2$)$_2$OTs, NaH, THF, 75 °C, 4 h, 88%. (c) TBAF, THF, 1 h, 93%. (d) i. TsCl, TEA, DCM, rt, 2 days; ii. NaN$_3$, DMF, 100 °C, 16 h, 95% over 2 steps. (e) DDQ, DCM/MeOH, in the dark, rt, 1 h, 60%. (f) *m*-CPBA, DCM, 4 °C, 18 h, 61%. (g) TEMPO/BAIB, DCM/^{t}BuOH/H$_2$O, 4 °C, 19 h, 89%. (h) i. Zn, NH$_4$Cl, MeOH/toluene, rt, 3 h; ii. Ac$_2$O, pyridine, DCM, 13 h, 13% over 2 steps. (i) i. Zn, NH$_4$Cl, MeOH/toluene, rt, 3 h; ii. (COCF$_3$)$_2$O, pyridine, DCM, 16 h, 36% over 2 steps. (j) Pd/C, H$_2$, MeOH, AcOH, rt, 5 h, 24%. (k) Pd/C, H$_2$, MeOH/dioxane, AcOH, rt, 5 h, 28%. (l) Na(s), NH$_3$, ^{t}BuOH, THF, −65 °C, 1 h, 31%.

ChemMedChem

Research Article
doi.org/10.1002/cmdc.202200580

Chemistry Europe
European Chemical
Societies Publishing

Pearlman's catalyst gave products **4** and **5** which were purified by reverse phase HPLC. Birch reduction of **12** in turn resulted in global debenzylation and azide reduction, yielding primary amine **3**.

ABPs **6** and **7** were synthesized in eight steps from partially protected *gluco*-configured cyclohexene **S2**[31] (Scheme 2). Trichloroacetimidation followed by stereospecific iodocyclisation led to 1,2-iodotrichloroimidate **15**, which was transformed stereospecifically into aziridine **16** by acidic hydrolysis of the imidate followed by aziridine ring-closure under mild basic conditions. Following installation of the 8-azido-octyl linker via *N*-alkylation of the unsubstituted aziridine, the primary alcohol in **17** was oxidized into carboxylic acid **18** using the Epp and Widlansky protocol as described above. Alternative oxidation attempts on a 4-*O*-debenzylated congener of **17** led to modest yields and to the formation of an aziridine-opened by-product (Table S1). The yield of the oxidation step could be improved by global benzyl protection of the secondary hydroxyl groups of the aziridine scaffold, as well as by purification of the oxidation product under neutral conditions and handling the compound at room temperature while removing volatiles. Next, removal of the benzyl groups and reduction of the azide into the corresponding primary amine was performed by dissolving-metal hydrogenolysis, providing highly polar species **19** with suitable purity after size-exclusion chromatography under mildly basic conditions. In the final step of the synthesis strategy, probes **6** and **7** were readily prepared via activation of the corresponding reporter into its pentafluorophenyl ester which was then reacted with the free amine in **19**. Reverse phase HPLC purification finally delivered the ABPs for ensuing application in competitive ABPP work. Overall, the number of synthetic steps towards β-D-glucuronidase ABPs starting from *gluco*-cyclohexene **S1** has been reduced to 9 steps while attaining moderately increased yields for both synthesized probes compared to previously reported strategy[20] (global yields in this work: 2.6% for **6**, 4.4% for **7**. In previous route,

global yields over 11 steps from **S1**: 2.4% for biotin-tagged ABP, 3.1% for Cy5-tagged ABP).

In vitro inhibition of recombinant β-D-glucuronidases

The newly synthesized inhibitors and ABPs **3**–**6** were next assessed for their inhibitory potency against representative recombinant *exo*- and *endo*-acting β-D-glucuronidases in comparison to *glucurono*-cyclophellitol **1** (Table 1). Inhibition was tested against microbial *Ec*GUS (an *Escherichia coli* GH2 *exo*-acting β-D-glucuronidase) and *Ac*GH79 (a GH79 β-D-glucuronidase from *Acidobacterium capsulatum* with *exo*- and *endo*-activity) by means of a fluorogenic substrate assay using 4-methylumbelliferyl β-D-glucuronide hydrolysis[21] as the read-out (Supporting Information Figures S2 and S3). The IC$_{50}$ values observed for *Ec*GUS inhibition are in line with what may be expected for this *exo*-acting enzyme: compound **6** (which features no substituent at *O*-4 and has the fluorescent reporter pointing in the direction of the aglycon of the natural substrate when bound in the enzyme active site) is a potent inhibitor whereas no inhibition was observed below 100 μM for 4-*O*-alkylated compounds **3**–**5**. In contrast, *Ac*GH79 was inhibited by **4** and **5** with nanomolar potency, underscoring this enzyme's *endo*-activity. Similar strong inhibition was observed for ABP **6**, while free amine **3** gave approximately two orders of magnitude lower inhibitory values compared to **4**. To assess the potency against recombinant HPSE, a gel-based competitive ABPP format was utilized with probe **7** as fluorescent read-out (Supporting Information Figure S4). Compounds **4** and **5** appeared to be roughly equally effective inhibitors, with potencies in the low micromolar range. Substitution of the naturally-occurring acetamide for the more lipophilic *N*-trifluoroacetyl group slightly increases HPSE inhibition. Cyclitol **3** does not inhibit HPSE up to 100 μM, a result that is in line with our previous finding that substitution of the GlcNAc moiety in compound **2** for glucosamine proved detrimental for HPSE inhibition. Altogether, these inhibitory data reveal that **4** and **5** are superior to *glucurono*-cyclophellitol in terms HPSE selectivity. In contrast, and matching results with our previous aziridine ABPs, ABP **6** proved to be moderately HPSE selective despite being a nanomolar inactivator of HPSE, due to its monosaccharide-like structure, and is therefore well suited for comparative

Scheme 2. Reagents and conditions: (a) CCl$_3$CN, DBU, DCM, rt, 2 h; then NIS, dry CHCl$_3$, 15 h, 0 °C→rt, 83%. (b) HCl in MeOH, DCM/MeOH 1:1, rt, 64 h; then Amberlite IRA-67, rt, 4 days, 87%. (c) 8-azido-octyl-trifluoromethanesulfonate, DIPEA, dry DCM, −10 °C→rt, 30 h, 85%. (d) TEMPO/BAIB, DCM/^{t}BuOH/H$_2$O, 0 °C→rt, 7 h, 60%. (e) Na, NH$_3$, ^{t}BuOH, −60 °C, 15 min, 84%. (f) i. Cy5-COOH, Pfp-TFA, DIPEA, DMF, 5 h; ii. **19**, DMF, rt, 18 h, 17% over 2 steps. (g) PEG$_3$-biotin-COOH, Pfp-TFA, DIPEA, DMF, 2 h 30 min; ii. **19**, DIPEA, DMF, rt, 24 h, 10% over 2 steps.

Table 1. β-D-Glucuronidase inhibition efficacy by 3–6.			
Inhibitor	IC$_{50}$ [μM] *Ec*GUS[a]	IC$_{50}$ [μM] *Ac*GH79[a]	IC$_{50}$ [μM] HPSE[b]	Selectivity factor[c]
1[d]	0.5 ± 0.1	0.033 ± 3·10^{-3}	> 100	N/A
3	> 100	21 ± 7	> 100	N/A
4	> 100	0.156 ± 6·10^{-3}	5 ± 2	20
5	> 100	0.167 ± 9·10^{-3}	1.5 ± 0.7	67
6	0.43 ± 0.07	1.43·10^{-3} ± 0.08·10^{-3}	0.2 ± 0.2	2
[a] 4-MU fluorogenic substrate assay. [b] In gel competitive ABPP-based assay. Reported values are mean ± S.D. of three technical replicates. [c] Calculated as ratio IC$_{50}$ *Ec*GUS/IC$_{50}$ HPSE. [d] Reported values are taken from the literature.[21,22]			

ChemMedChem

Research Article
doi.org/10.1002/cmdc.202200580

Chemistry
Europe

European Chemical
Societies Publishing

and competitive ABPP studies in which both *exo*- and *endo*-β-D-glucuronidase activities are interrogated.

Structural characterization of enzyme-ligand interactions

We next sought to examine how **3–5** bind to the enzymatic site of *endo*-acting β-D-glucuronidases by X-ray diffraction of co-crystal structures of these ligands with *Ac*GH79 and HPSE. For both enzymes, we found density for covalent adducts of **4** (Figure 4A and S6) and **5** (Figure 4C and S7) bound to the catalytic nucleophile, consistent with nucleophilic ring-opening of the epoxide. Reacted inhibitors adopted a $^4C_1$ covalent intermediate conformation, in agreement with the canonical retaining β-D-glucuronidase conformational itinerary followed by these enzymes. In particular, the crystal structure of HPSE bound to **4** showed an H-bond network involving the acetamide moiety with residues D62 and Y391. This binding pose is also observed for compound **5** featuring a trifluoroace-tamide. Interestingly, inhibitor **5** displays a second energeti-cally-equivalent binding mode, in which the *N*-trifluoroacetyl-ethylene substitution is oriented away from Y391. Thus, in this additional binding modality the trifluoroacetamide group is precluded from interaction with Y391 and interacts instead with nearby N64. We reason that this is caused by the fact that the trifluoroacetamide (as in **5**) has weaker H-bond donating capacity when compared to the acetamide (as in **4**). Soaking crystals of *Ac*GH79 or HPSE with **3** did not result in ligand-enzyme crystal complexes, which is in line with the *in vitro* IC$_{50}$ value we obtained for this compound (no inhibition up to 100 μM).
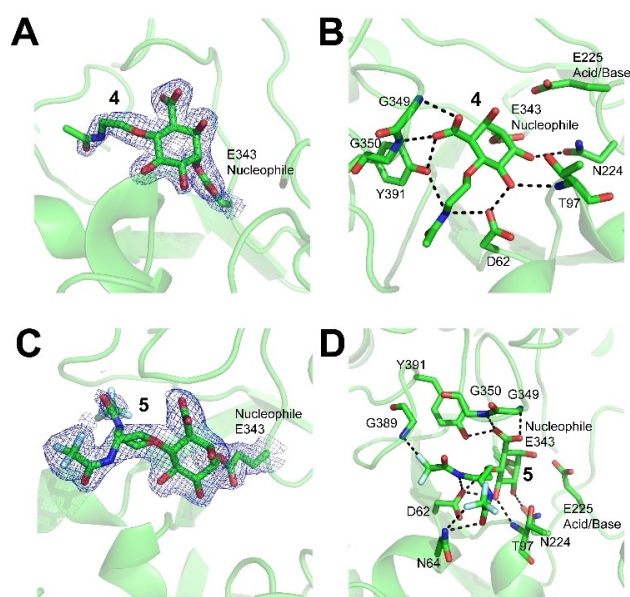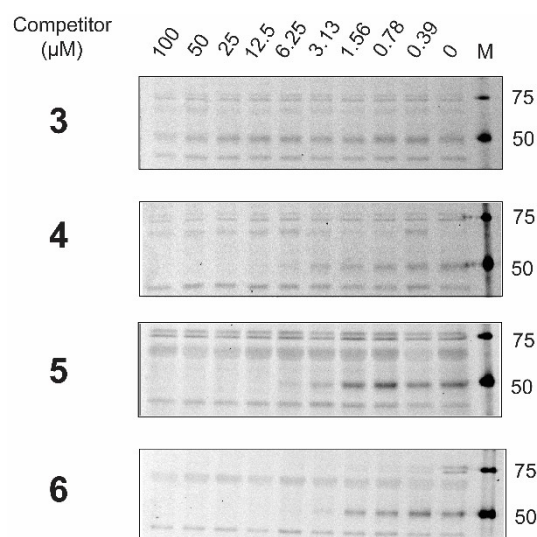
Figure 5. *In vitro* HPSE selectivity by **3–6** in platelet lysates as determined by competitive ABPP in blood platelet lysate. Fluorescent labelling of HPSE by **7** can be abrogated by pre-incubation with inhibitors **4** and **5** without altering GUSB signal, thus demonstrating the selectivity of compounds **4** and **5** for human HPSE in the presence of this *exo*-acting β-D-glucuronidase. In contrast, **3** does not inhibit GUSB nor human HPSE below 100 μM.

Inhibitory activity in blood platelet extracts

To establish the β-D-glucuronidase inhibitory activity of **3–6** in complex biological samples, we included these in a competitive ABPP assay in blood platelet lysate (Figure 5) using ABP **7**, which labels both GUSB (two isoforms at 75–78 kDa) and HPSE (58 kDa) in this material, as the readout. We chose blood platelets because of the high levels of HPSE expression occurring in these cells.[32–34] Preincubation with **3–6** at increasing concentrations up to 100 μM at pH 5.0 for 60 minutes was followed by treatment with **7** (100 nM) for 30 minutes, after which the samples were resolved with SDS-PAGE and ABP **7**-modified GUSB/HPSE detected by fluorescence scanning of the wet gel slabs. Fluorescent labeling of HPSE was abrogated by competition with **4** or **5** without altering GUSB signal at the tested concentrations, thus demonstrating the ability of these compounds to selectively inhibit HPSE over GUSB in the low-micromolar range also in these samples. In contrast, biotin-ABP **7** showed complete deletion of GUSB bands down to 390 nM and deletion of HPSE band up to 3 μM, proving its superior GUSB selectivity, whereas free amine **3** proved inactive against both enzymes.

Conclusion

In this work we show that 4-*O*-alkyl glucuronic cyclophellitols, which are structurally more accessible than the GlcNAcylated ones we reported previously, are *bona fide* and selective mechanism-based HPSE inhibitors able to disable the target enzyme also in complex biological samples: extracts from blood platelets. In view of the importance of HPSE as antimetastatic

Figure 4. Crystal structures of reacted **4** (**A** and **B**) and **5** (**C** and **D**) with HPSE at 1.95 Å and 2.0 Å resolution, respectively. Electron densities (**A** for **4**, **C** for **5**) and H-bond interactions (**B** for **4**, **D** for **5**) are depicted.

drug target, and the current interest of mechanism-based enzyme inhibitors in drug discovery and development,[35] we believe our results represent a step forward in the design of more selective HPSE inhibitors. This paper also describes methodologies that support further optimization of the cyclophellitol leads and their assessment in more advanced biological models. This includes a versatile ABPP toolkit, including a more efficient synthesis of both a fluorescent ABP (for in gel competitive ABPP as shown here) and a biotinylated one (for future use in target engagement studies in *in vivo* models) that report on both *exo-* and *endo*-acting β-D-glucuronidases. In addition, our structural work reveals the importance of the acetamide moiety that characterizes two of our inhibitors and also that of the (synthetically more involved) disaccharide that we reported[22] recently. This will assist in further optimizing the structure of HPSE inhibitors: by adding substituents that may increase enzyme active site binding (and thus inhibitory potency) but also subtracting redundant functionalities so as to create structurally even more simple compounds. These strategies can aid in the progress towards the design of new HPSE inhibitors with clinical potential, thereby bringing the concept of mechanism-based inhibitors as clinical drugs/drug candidates also to the field of glycobiology/glycoprocessing enzymes.

Experimental Section

Materials

Chemicals were purchased from Acros, Sigma Aldrich, Biosolve, VWR, Fluka, Merck and Fisher Scientific and used as received unless stated otherwise. Tetrahydrofuran (THF), dichloromethane (DCM), *N,N*-dimethylformamide (DMF) and toluene were stored over molecular sieves before use.

Synthesis

All reactions were performed under an argon atmosphere unless stated otherwise. TLC analysis was conducted using Merck aluminum sheets. Reaction conditions and characterization data of synthetic intermediates and of final products by ^{1}H and ^{13}C NMR and HR-MS spectrometry are provided in the Supporting Information.

Determination of *in vitro* apparent IC$_{50}$ values

IC$_{50}$ values against recombinant EcGUS and *Ac*GH79 were determined by an enzymatic fluorescence assay method using fluorogenic substrate 4-methylumbelliferyl-β-D-glucuronide (4-MU-β-GlcA).[20] IC$_{50}$ values against recombinant HPSE were assessed by in-gel competitive ABPP using ABP **7** as fluorescent readout (Supporting Information).

Calculation of FEL

FELs of unsubstituted *glucurono*-cyclophellitol and cyclophellitol were modelled *in vacuo* using Density Functional Theory (DFT)-based molecular dynamics, using the Car-Parrinello method (Supporting Information).

Conflict of Interest

The authors declare no conflict of interest.

Data Availability Statement

The data that support the findings of this study are available in the supplementary material of this article.

Keywords: cyclitols · carbohydrates · inhibitors

[1] S. Sarrazin, W. C. Lamanna, J. D. Esko, *Cold Spring Harbor Perspect. Biol.* **2011**, *3*, a004952.
[2] U. Häcker, K. Nybakken, N. Perrimon, *Nat. Rev. Mol. Cell Biol.* **2005**, *6*, 530–541.
[3] J. Winkler, A. Abisoye-Ogunniyan, K. J. Metcalf, Z. Werb, *Nat. Commun.* **2020**, *11*, 5120.
[4] L. Wu, C. Viola, A. Brzozowski, G. J. Davies, *Nat. Struct. Mol. Biol.* **2015**, *22*, 1016–1020.
[5] K. M. Jayatilleke, M. D. Hulett, *J. Transl. Med.* **2020**, *18*, 453–478.
[6] I. Boyango, U. Barash, I. Naroditsky, J. P. Li, E. Hammond, N. Ilan, I. Vlodavsky, *Cancer Res.* **2014**, *74(16)*, 4504–4514.
[7] B. Tang, R. Xie, Y. Qin, Y. Xia, X. Yong, L. Zheng, H. Dong, S. Yang, *Oncotarget* **2016**, *7*, 11364–11379.
[8] I. Vlodavsky, Y. Friedmann, *J. Clin. Invest.* **2001**, *108*, 341–347.
[9] M. Elkin, N. Ilan, R. ishai-Michaeli, Y. Friedmann, O. Papo, I. Pecker, I. Vlodavsky, *FASEB J.* **2001**, *15*, 1661–1663.
[10] J. P. Ritchie, V. C. Ramani, Y. Ren, A. Naggi, G. Torri, B. Casu, S. Penco, P. Carminati, M. Tortoreto, F. Zunino, I. Vlodavsky, R. D. Sanderson, Y. Yang, *Clin. Cancer Res.* **2011**, *117*, 1382–1393.
[11] H. Zhou, S. Roy, E. Cochran, R. Zouaoui, C. L. Chu, J. Duffner, G. Zhao, S. Smith, Z. Galcheva-Gargova, J. Kalgren, N. Dussault, R. Y. Q. Kwan, E. Moy, M. Barnes, A. Long, C. Honan, Y. W. Qi, Z. Shriver, T. Ganguly, B. Schultes, G. Venkataraman, T. K. Kishimoto, *PLoS One* **2011**, *6*, 6, e21106.
[12] C. R. Parish, C. Freeman, K. J. Brown, D. J. Francis, W. B. Cowden, *Cancer Res.* **1999**, *59*, 3433–3441.
[13] V. Ferro, L. Liu, K. D. Johnstone, N. Wimmer, T. Karoli, P. Handley, J. Rowley, K. Dredge, C. P. Li, E. Hammond, K. Davis, L. Sarimaa, J. Harenberg, I. Bytheway, *J. Med. Chem.* **2012**, *55*, 3804–3813.
[14] D. R. Coombe, N. S. Gandhi, *Front. Oncol.* **2019**, *9*, 1316.
[15] M. Sue, N. Higashi, H. Shida, Y. Kogane, Y. Nishimura, H. Adachi, E. Kolaczkowska, M. Kepka, M. Nakajima, T. Irimura, *Int. Immunopharmacol.* **2016**, *35*, 15–21.

[16] H. Umezawa, T. Aoyagi, T. Komiyama, H. Morishima, M. Hamada, T. Takeuchi, *J. Antibiot.* **1974**, *27*, 963–969.

[17] P. A. Driguez, M. Petitou, **2005**, EP1773854B1 (patent).

[18] A. Palumbo, A. Larocca, M. Genuardi, K. Kotwica, F. Gay, D. Rossi, G. Benevolo, V. Magarotto, F. Cavallo, S. Bringhen, C. Rus, L. Masini, M. Iacobelli, G. Gaidano, C. Mitsiades, K. Anderson, M. Boccadoro, P. Richardson, *Haematologica* **2010**, *95*, 1144–1149.

[19] H. Li, H. Li, H. Qu, M. Z. Zhao, B. Yuan, M. H. Cao, J. Q. Cui, *Cancer Cell Int.* **2015**, *15*, 52–62.

[20] V. N. Madia, A. Messore, L. Pescatori, F. Saccoliti, V. Tudino, A. De Leo, M. Bortolami, L. Scipione, R. Costi, S. Rivara, L. Scalvini, M. Mor, F. F. Ferrara, E. Pavoni, G. Roscilli, G. Cassinelli, F. M. Milazzo, G. Battistuzzi, R. Di Santo, G. Giannini, *J. Med. Chem.* **2018**, *61*, 6918–6936.

[21] L. Wu, J. Jiang, Y. Jin, W. W. Kallemeijn, C.-L. Kuo, M. Artola, W. Dai, C. van Elk, M. van Eijk, G. A. van der Marel, J. D. C. Codée, B. I. Florea, J. M. F. G. Aerts, H. S. Overkleeft, G. J. Davies, *Nat. Chem. Biol.* **2017**, *13*, 867–873.

[22] C. de Boer, Z. Armstrong, V. A. J. Lit, U. Barash, G. Ruijgrok, I. Boyango, M. M. Weitzenberg, S. P. Schröder, A. J. C. Sarris, N. J. Meeuwenoord, P. Bule, Y. Kayal, N. Ilan, J. D. C. Codée, I. Vlodavsky, H. S. Overkleeft, G. J. Davies, L. Wu, *Proc. Natl. Acad. Sci. USA* **2022**, *31*, 119, e2203167119.

[23] L. Wu, J. Jiang, N. Wimmer, G. J. Davies, V. Ferro, *Chem. Commun.* **2020**, *56*, 13780–13783.

[24] K. LI, J. Jiang, M. D. Witte, W. W. Kallemeijn, W. E. Donker-Koopman, R. G. Boot, J. M. F. G. Aerts, J. D. C. Codée, G. A. van der Marel, H. S. Overkleeft, *Org. Biomol. Chem.* **2014**, *12*, 7786–7791.

[25] D. E. Koshland, *Biol. Rev. Cambridge Philos. Soc.* **1953**, *28*, 416–436.

[26] A. Laio, M. Parrinello, *Proc. Natl. Acad. Sci. USA* **2002**, *99*, 12562–12566.

[27] D. Cremer, J. A. Pople, *J. Am. Chem. Soc.* **1975**, *97*, 1354–1358.

[28] A. Ardèvol, C. Rovira, *J. Am. Chem. Soc.* **2015**, *137(24)*, 7528–7547.

[29] F. G. Hansen, E. Bundgaart, R. Madsen, *J. Org. Chem.* **2005**, *70*, 10139–10142.

[30] J. B. Epp, T. S. Widlanski, *J. Org. Chem.* **1999**, *64(1)*, 293–295.

[31] T. J. M. Beenakker, D. P. A. Wander, J. D. C. Codée, J. M. F. G. Aerts, G. A. van der Marel, H. S. Overkleeft, *Eur. J. Org. Chem.* **2018**, *20–21*, 2504–2517.

[32] A. Eldor, N. Bar-Ner, J. Yahalom, Z. Fuks, I. Vlodavsky, *Semin. Thromb. Hemostasis* **1987**, *13(4)*, 475–478.

[33] C. Freeman, C. R. Parish, *Biochem. J.* **1998**, *330*, 1341–1350.

[34] R. Ishai-Michaeli, A. Eldor, I. Vlodavsky, *Cell Regul.* **1990**, *1*, 833–842.

[35] F. Sutanto, M. Konstantinidou, A. Domling, *RSC Med. Chem.* **2020**, *11*, 876–884.